Relation between the degree and betweenness centrality distribution in complex networks

H. Masoomy,[1] V. Adami,[2] and M. N. Najafi[2,*]
[1]*Department of Physics, Shahid Beheshti University, 1983969411 Tehran, Iran*
[2]*Department of Physics, University of Mohaghegh Ardabili, P.O. Box 179, Ardabil, Iran*

(Received 29 April 2022; revised 9 September 2022; accepted 7 March 2023; published 17 April 2023)

The centrality measures, like betweenness b and degree k in complex networks remain fundamental quantities helping to classify them. It is realized from Barthelemy's paper [Eur. Phys. J. B **38**, 163 (2004)] that the maximal $b-k$ exponent for the scale-free (SF) networks is $\eta_{\max}=2$, belonging to SF trees, based on which one concludes $\delta \geqslant \frac{\gamma+1}{2}$, where γ and δ are the scaling exponents for the distribution functions of the degree and the betweenness centralities, respectively. This conjecture was violated for some special models and systems. Here we present a systematic study on this problem for visibility graphs of correlated time series, and show evidence that this conjecture fails in some correlation strengths. We consider the visibility graph of three models: two-dimensional Bak-Tang-Weisenfeld (BTW) sandpile model, one-dimensional (1D) fractional Brownian motion (FBM), and 1D Levy walks, the two latter cases are controlled by the Hurst exponent H and the step index α, respectively. In particular, for the BTW model and FBM with $H \lesssim 0.5$, η is greater than 2, and also $\delta < \frac{\gamma+1}{2}$ for the BTW model, while the Barthelemy's conjecture remains valid for the Levy process. We assert that the failure of the Barthelemy's conjecture is due to large fluctuations in the scaling $b-k$ relation resulting in the violation of hyperscaling relation $\eta = \frac{\gamma-1}{\delta-1}$ and emergent anomalous behavior for the BTW model and FBM. Universal distribution function of generalized degree is found for these models which have the same scaling behavior as the Barabasi-Albert network.

DOI: 10.1103/PhysRevE.107.044303

I. INTRODUCTION

Among many general measures for the centrality in the complex networks which have been devised to quantify the role and the importance of nodes, and also to identify how much effect the nodes have on the network properties, the betweenness, and the degree centralities are at the center of much attention. Consider a network in which the *agents* (which are the nodes in the network) choose the shortest paths for the interaction to optimize efficiency. Then a central role is granted to a node that is visited with a high frequency in the possible interactions, which is expressed via the *betweenness centrality*, defined for a node i as

$$b_i = \sum_{i\neq m\neq n} \sigma_{m,n}(i)/\sigma_{m,n}, \tag{1}$$

where $\sigma_{m,n}$ $[\sigma_{m,n}(i)]$ is the total number of shortest paths from node m to node n (through i). This is something different from the *degree centrality* which deals with how interactive the agents are based on the number of their local connections, and is defined as

$$k_i = \sum_j A_{ij}, \tag{2}$$

where the adjacency matrix A_{ij} is 1 when the nodes i and j are connected and zero otherwise. Other centralities, like the eigenvector, the closeness, and the subgraph centralities are defined by focusing on the other properties of the networks; see Ref. [1] for details. The *clustering coefficient* of node i is defined by

$$c_i = 2\left(\sum_{i\neq m\neq n} A_{im}A_{in}A_{mn}\right) \Big/ [k_i(k_i-1)]. \tag{3}$$

The degree and the betweenness centralities apply to a broad range of systems like the social networks, biology, scientific cooperation, and transport. A huge number of numerical [2–4] and analytical [5–7] studies have concentrated on these centralities for various complex systems, like the scale-free (SF) networks which is much more interesting in the sense of power-law behavior with scaling exponents allowing one to classify the models into universality classes. The leading examples of power-law distributions are associated with the degree and betweenness of nodes, i.e., (up to some cutoff values)

$$p(k) \propto k^{-\gamma} \text{ and } p(b) \propto b^{-\delta}, \tag{4}$$

where γ (usually in the interval [2,3]) and δ are called the degree and the betweenness exponents, respectively. These exponents (which are not generally independent) serve as leading measures for classifying the SF networks [1]. As a well-known fact for SF networks, when the conditional probability distribution $p(b|k)$ is a peaked narrow function of both k and b, then

$$b \propto k^{\eta}, \tag{5}$$

*morteza.nattagh@gmail.com

with a hyperscaling relation [8]

$$\eta = \frac{\gamma - 1}{\delta - 1}, \tag{6}$$

a relation that is violated when the fluctuations are high so that $p(b|k)$ is not a narrow function. These large fluctuations (and the violation of the above relation) results in many interesting aspects in complex networks. An example is a nonmonotonic relation between b and k, e.g., a node with a high degree centrality is not necessarily an important node in the sense of betweenness [9–13], which itself leads to failure of the mean field (MF) arguments. This phenomena leads also to the *fractal networks*, or *fractality* observed in the synthetic and real-world SF networks [11]. Therefore it always has been worth investigating the theoretical relation between b and k, and also between other observables, and depends on the structure of SF networks. It was conjectured by Goh *et al.* [3] that the amount of δ is robust and can be used to classify SF networks, based on which two universality classes were proposed $\delta = 2.2(1)$ (for the protein-interaction networks, the metabolic networks for eukaryotes and bacteria, and the co-authorship network), and $\delta = 2.0$ [for the Internet, the World Wide Web (WWW), and the metabolic networks for Archaea] [3,14]. The hyperscaling relation between γ and δ is important to reduce the number of independent critical exponents which is critical in identifying the determination of the universality classes. Barthelemy argued that the Goh's conjecture is questionable since δ varies continuously as a function of γ in many networks. Indeed, Barthelemy concluded that the only restrictions that the exponents have are [7,15]

$$(\mathrm{C}\mathbb{I}) : \eta_{\max} = \eta_{\mathrm{SFT}} = 2, \quad (\mathrm{C}\mathbb{I}\mathbb{I}) : \delta \geqslant \frac{\gamma + 1}{2}, \tag{7}$$

where SFT stands for scale-free trees. The first equation (C$\mathbb{I}$) states that η is maximal for SFTs and the inequality (C$\mathbb{I}\mathbb{I}$) is based on Eq. (6) for $\eta_{\max}$ (the equality holds for SFTs).

Equation (C$\mathbb{I}$) serves as an important difference between SF networks and SFTs. Large $b - k$ fluctuations [and consequently a violation of Eq. (6)] is a source of anomalous behavior explored above, and also the MF arguments that has led to the Barthelemy's conjecture Eq. (7). This conjecture was violated for some special models and systems. Especially Eq. (C$\mathbb{I}$), which naturally results in Eq. (C$\mathbb{I}\mathbb{I}$). There are some reports that show this is the case for realistic situations. In Ref. [16] an η larger than 2 was reported for VGs reconstructed from earthquake magnitude time series of three regions, Italy (2.92), Southern California (2.59), and Mexico (2.89).

In this paper we present a systematic study on this problem for visibility graphs and show evidence that this conjecture breaks down in some domain of correlations. We think that it helps much to figure out the scenarios explaining these observations. We show that Barthemely's conjecture Eq. (7) is highly restricted for SF visibility graphs (VGs). We assert and numerically demonstrate that it is due to the large $b - k$ fluctuations.

The paper is organized as follows: In the next section we describe the VG method. In Sec. II we present some arguments about the consequences of the Barthelemy's conjecture. Section III B is devoted to correlated time series that are investigated in this work. The numerical results are presented in Sec. IV. We close the paper by a conclusion.

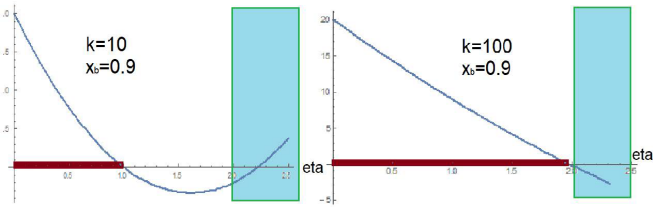

FIG. 1. $f(\eta, k, x_b)$ in terms of η for $x_b = 0.9$ and $k = 10$ (left) and $k = 100$ (right). The allowed values for η is given by $f(\eta, k, x_b) \geqslant 0$, highlighted by red bar on the horizontal axis. The azure rectangle area shows the forbidden η values with $\eta > 2$ according to Eq. (7).

II. ARGUMENTS ON BARTHELEMY'S RELATION

There is no rigorous proof for (C$\mathbb{I}$) in Eq. (7), and the arguments that lead to it are based on an argument presented in Ref. [7] in which it is first argued that for trees $\eta = 2$. Then, since all shortest paths should pass a typical node in trees, it is asserted that the maximal betweenness centrality is for trees. While the argument is correct, the conclusion seems not to be general enough, since the fact that betweenness centrality for trees is higher than other networks, the exponent η is related to the slope of the $b - k$ graphs not the local values. In this paper we show that for the VGs the equation (C$\mathbb{I}$) is also violated for some correlated time series.

The Eq. (7) results in another important identity for large b and k values. The details of the calculations is presented in Appendix A. Most importantly, the Eq. (7) implies that [Eq. (A6) and (A7)]

$$f(\eta, k, x_b) \geqslant 0, \tag{8}$$

where

$$f(\eta, k, x_b) \equiv x_b\eta^2 - [k + 1 - (k - 1)x_b]\eta + 2k(1 - x_b). \tag{9}$$

In this equation $x_k \equiv \frac{p(k+1)}{p(k)}$, $x_b \equiv \frac{p(b_{k+1})}{p(b_k)}$. This function has been shown in Fig. 1 for two different k values. The failure of Eq. (7) results to the failure of the above identities. The interval of η that is compatible with Berthelemy's conjecture is

$$\begin{cases} \eta > \eta_*^{(+)} \\ \eta < \eta_*^{(-)}, \end{cases} \text{combined with } \eta \leqslant 2, \tag{10}$$

where $\eta_*^{(\pm)}$ are given by [Eq. (A8)]

$$\eta_*^{\pm} = (2x_b)^{-1}[B \pm \sqrt{B^2 + 8kx_b(1 - x_b)}],$$
$$B = k + 1 - (k - 1)x_b. \tag{11}$$

In the limit $k \to \infty$, the condition (C$\mathbb{I}$) is retrieved. The upper branch $\eta_*^{(+)}$ grows linearly with k for large enough k values, while the lower branch saturates to $\eta_*^{(-)} \to 2$. Therefore, for $k \to \infty$, the solution $\eta < 2$ is the exact solution as expected. To see this more directly, notice that

$$f(\eta, k, x_b)|_{k\to\infty} \to k(1 - x_b)(2 - \eta), \tag{12}$$

so that $f(\eta, k, x_b) \geqslant 0$ (noting that $0 < x_b < 1$) gives $\eta \leqslant 2$. As another example, consider the case η is about 2, i.e., $\eta = 2^-$, where Eq. (A6) for finite and large k values imply that [to $O(k^{-2})$]

$$\frac{1}{x_b} \leqslant \eta - 1 < 1. \tag{13}$$

Therefore, the prediction of the Barthelemy's conjecture in this case (η close to two) is

$$x_b \geqslant \frac{1}{\eta - 1}. \tag{14}$$

Therefore, for the η values close to two, one finds that $x_b \geqslant \frac{1}{\eta-1}$ [to $O(k^{-2})$].

III. VISIBILITY GRAPH OF CORRELATED TIME SERIES

Visibility graph (VG) method is a tool to convert a given time series to a network, and plays an essential role in understanding the properties of nonlinear dynamical systems. A high degree centrality of a node in VGs reflects a good *visibility* of that node showing that it is a hub, while a high betweenness centrality of a given node i shows that this node not only is a hub but has a sufficient distance from a next hub, i.e., it is rare.

A. Visibility graph definition

We consider a time series $\{s(t_i)\}_{i=1}^N$, where s is called the *activity* here, and N is a maximal time in the analysis, and is also the size of the VG. The VG denoted by $G(V, E)$ is a network in which the nodes $V = \{v_i\}_{i=1}^N$ represent the times $T = \{t_i\}_{i=1}^N$, such that $v_i = t_i$ and $E \subseteq V \times V$ is the set of links connecting the nodes, such that the nodes v_i and v_j are connected $(v_i, v_j) \in E$, if and only if their corresponding data points $s(v_i)$ and $s(v_j)$ are visible to each other. More practically, to each time in the time series we attribute a node, and the connection between two nodes is established if the associated activities are visible to each other, i.e., the is no node between them that is high so that two nodes do not "see" each other. The adjacency matrix for VG is defined by

$$A_{ij} = \begin{cases} \prod_{k=i+1}^{j-1} \Theta(s_{ij} - s_{ik}) & \text{if } |t_i - t_j| > 1 \\ 1 & \text{if } |t_i - t_j| = 1, \end{cases} \tag{15}$$

where

$$s_{mn} \equiv \frac{s(t_n) - s(t_m)}{t_n - t_m}, \tag{16}$$

and Θ is the step function that satisfies the visibility condition [17].

Many statistical observables like the clustering coefficient, mean length of the shortest paths and motif distribution as well as assortative mixing pattern were studied in Ref. [18], and a homological analysis can be found in Ref. [17], showing that the natural VGs are the topological tree. Many statistical [19] and topological [17] aspects of VGs have been studied numerically and analytically, making it a standard powerful tool to study various systems like earthquakes [16], economics [20], ecology [21], neuroscience [22,23], and biology [24]. An important step toward understanding of the scaling properties of VGs was taken by Lacasa, who showed that a self-similar time series converts to a SF network, emphasizing that the power-law degree distributions are related to fractality [19,25]. Some time series are shown in Fig. 2 to be described in the next section.

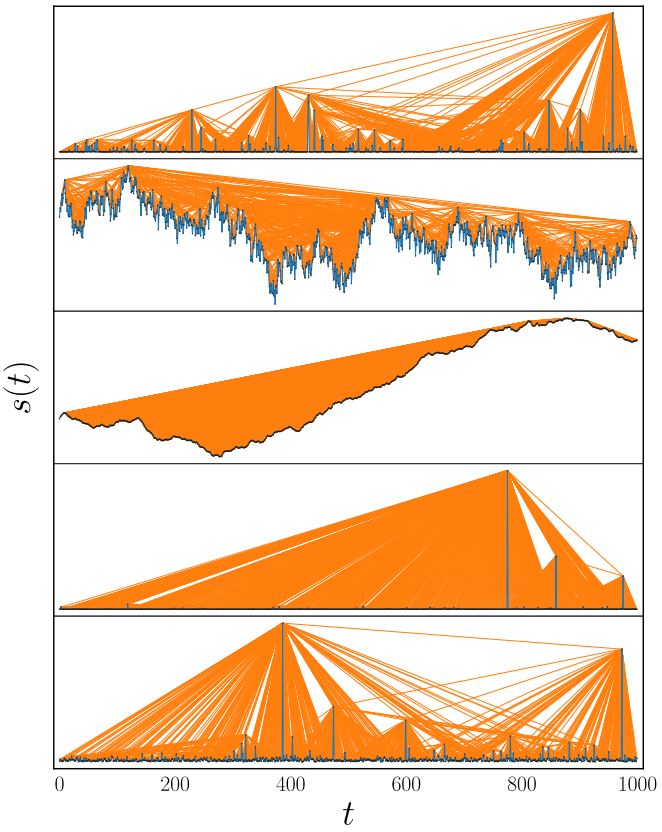

FIG. 2. Visibility graphs constructed from the time series (blue curve) of various process studied in this work. BTW model (top panel), FBM series $H = 0.2$ (middle-top panel), FBM series $H = 0.8$ (middle panel), Levy walk $\alpha = 0.9$ (middle-bottom panel), and Levy walk $\alpha = 1.6$ (bottom panel). Data points (nodes) are represented by black dots and visibility lines (links) are shown by orange lines.

B. Correlated times series

Here we systematically study the VGs for three following general processes which are representatives of leading classes in statistical mechanics and nonlinear systems, namely, the BTW sandpile model, one-dimensional (1D) fractional Brownian motion (fBM), and 1D Levy processes.

(i) *2D BTW sandpile model*. This model explains the avalanche dynamics as the main building block of self-organized critical systems like real sandpiles [26], earthquakes [27], sun flares [28], forest fire [29], cumulus clouds [30], Barkhausen effect in superconductors [31], and rainfall [32]. BTW model on a square $L \times L$ lattice is defined by a height variable $h_i \in [1, 4]$, which is increased upon adding a grain to a random site i so that $h_i \to h_i + 1$. If $h_i > 4$, a toppling process starts according to which four grains leave i and each neighboring site rise by one unit (toppling). For the boundary sites one or two sand grains are lost. An avalanche is defined

as the chain of the activity between two stable states. After a size-dependent timescale, the system enters into a state where the number of wasted grained are more or less equal to the number of injected grains, called the *stationary regime*. We study this model in the stationary regime, see Ref. [32] for details. The time series of interest here is the size of avalanches $s(t)$, defined as the number of local topplings in an avalanche.

(ii) *1D fractional Brownian motion (fBM).* This model is a popular model for both short-range and long-range dependent phenomena in various fields, including physics, biology, hydrology, network research, financial mathematics, etc. [33]. fBM is controlled by the *Hurst exponent H* defined using the relation

$$s_H(t) = \frac{1}{\Gamma(H+1/2)} \int_0^t (t-t')^{H-1/2} ds_B(t'), \tag{17}$$

where $s_B(t)$ is the standard 1D Brownian motion. It has been numerically has shown that for the VG of FBM and fractional Gaussian noise (FGN), γ varies linearly with H as [25]

$$\begin{aligned} \gamma_{\rm fBM}(H) &= a_{\rm fBM} - b_{\rm fBM} H, \\ \gamma_{\rm fGN}(H) &= a_{\rm fGN} - b_{\rm fGN} H, \end{aligned} \tag{18}$$

respectively, where it was conjectured that the constants are $a_{\rm fBM} = 3$, $b_{\rm fBM} = 2$, $a_{\rm fGN} = 5$, and $b_{\rm fGN} = 2$. This relation was further improved in Ref. [34] by $a_{\rm fBM} = 3.35$, $b_{\rm fBM} = 2.87$.

(iii) *1D Levy process.* This model is a prototype of time-correlated self-similar systems, defined by random flights for which the step size s follows a power-law probability density function, $p(s) \propto s^{-1-\alpha}$,where α is the *step index* tuning the correlations. The Levy distribution has a long-range algebraic tail corresponding to large but infrequent steps, so-called *rare events*. For $\alpha < 2$ the mean square deviation diverges with the dynamic exponent α (superdiffusion), for which the dominant behavior is dictated by the rare events over long times [35].

For an illustration of VG constructed by time series, we plot time series (blue curves) that were used in this paper (BTW, $\text{FBM}_{H=0.2}$, $\text{FBM}_{H=0.8}$, $\text{Levy}_{\alpha=0.9}$, and $\text{Levy}_{\alpha=1.6}$ from top to bottom), along with the nodes (black dots) and links (orange lines) in Fig. 2. For the fBM series by increasing the Hurst exponent H, the data points gain more chance to be visible by each other, and consequently the VGs corresponding to the correlated fBMs are denser than the anticorrelated ones. The situation is different for the Levy process, i.e., the Levy flights associated with the small step index α values contain many rare events having good visibility condition which makes the associated VG dense.

IV. RESULTS

In this section we present the results of the simulations. The BTW model was simulated in $L \times L$ square lattice. To control the finite-size effects, we considered $L = 64, 128, 256, 512, 1024$, and 2048. The size of the time series for all of the models was considered to be $\frac{N}{10^3} = 1, 2, 4, 8$, and 16 (for the BTW model $\frac{N}{10^3} = 32, 64$ are added). For simulating of the Levy process is determined by two parameters: the step index α (explained above), and skewness parameter β which (zero in this paper), the location parameter (zero in this paper), and the scale parameter (unity in this paper), see Eq. [8] of the Ref. [36].

An important check for the growing SF networks is concerning their dynamic scaling properties, helping to identify their universality classes. We first consider the generalized degree $q_i(t) \equiv \sqrt{t_i} k_i(t)$, where t_i is the birth time of the node v_i. For the Barabasi-Albert networks (m-BA network, where m is the number of new links established upon adding a new node, so that $m = 1$ generates a tree) the dynamic distribution function of q satisfies [37]

$$p(q,t) = t^{-\frac{1}{2}} F_{\rm BA}^{(m)}\left(q\, t^{-\frac{1}{2}}\right), \tag{19}$$

where $F_{\rm BA}^{(m)}(\xi)$ is an m-dependent universal function. This function exhibits the following asymptotic behavior [37],

$$F_{\rm BA}^{(m)}(\xi) \propto \begin{cases} \xi^{\phi_m}; & \xi \ll \xi_m \\ \exp\left[-a_m \xi\right]; & \xi \gg \xi_m, \end{cases} \tag{20}$$

where $\phi_{m=1} = 2$, $\phi_{m>1} \approx 2.9$, $a_{m=1} \approx 1.4$, $a_{m>1} \approx 2.5$, $\xi_{m=1} = 2$, and $\xi_{m>1} \approx 1.5$.

For the models considered in this paper, although the universal functions are quite different, the same dynamic scaling exponents are observed. More precisely, the data collapse analysis depicted in Figs. 3 (top row) shows the same scaling exponents ($\frac{1}{2}$ and $\frac{1}{2}$) as Eq. (19). Importantly, the exponents do not depend on H and α for fBM and Levy processes, respectively, showing that these exponents are superuniversal. The universal functions $F_{\rm BTW}(\xi)$, $F_{\rm fBM}(\xi)$, and $F_{\rm Levy}(\xi)$ are all linearly increasing functions of ξ for small enough ξ, demonstrating that $p(q,t) \propto t^{-1} q$ for small $t^{-1} q$ values. For the models considered in this paper, we found convincing evidence that the universal function, behaves asymptotically like (apart from some jumps, i.e., the discontinuities)

$$F_{\rm x}(\xi) \propto \begin{cases} \xi^{\phi_{\rm x}}; & \xi \ll \xi_{\rm x} \\ (\ln \xi)^{-\psi_{\rm x}}; & \xi \gg \xi_{\rm x}, \end{cases} \tag{21}$$

where x stands for BTW, fBM, and Levy, and $\xi_{\rm x}$ is a crossover point. These behaviors are depicted in Fig. 3 (bottom figures). Within our numerical errors, the exponents consistent with $\phi_{\rm BTW} = 0.9359 \pm 0.0081$, $\phi_{\rm fBM} = 0.9653 \pm 0.0054$, $\phi_{\rm Levy} = 0.9485 \pm 0.0075$, $\psi_{\rm BTW} = 7.82 \pm 0.02$, $\psi_{\rm fBM} = 4.88 \pm 0.03$, $\psi_{\rm Levy} = 5.22 \pm 0.03$, $\xi_{\rm BTW} \approx 3$, and $\xi_{\rm fBM} \approx \xi_{\rm Levy} \approx 2$.

To assess the Barthemly's conjecture we consider the behavior of k as well as b, and the relation between them. In the Fig. 4 we show the $b-k$ (first row), $c-k$ (middle row), and $b-c$ (bottom row) scaling relations. In each row, the finite-size scaling of results of the BTW (first column), fBM (middle column), and Levy (third column) processes are shown. The insets show the behavior of η in terms of the system size (N and L for the BTW model, and N for the others). The b-k relation in the log-log scale for the fBM is not as straight as the other cases. For extracting the exponents, we picked the straight part of the graph (ignored the first and the end part of the graph) to reach a specified accuracy, i.e., $R^2 = 0.99$. First observe that the data in the $b-k$ diagrams are properly collapsed showing the following finite-size scaling for *all models*

$$b \propto N^{-\beta\eta} k^{\eta}, \tag{22}$$

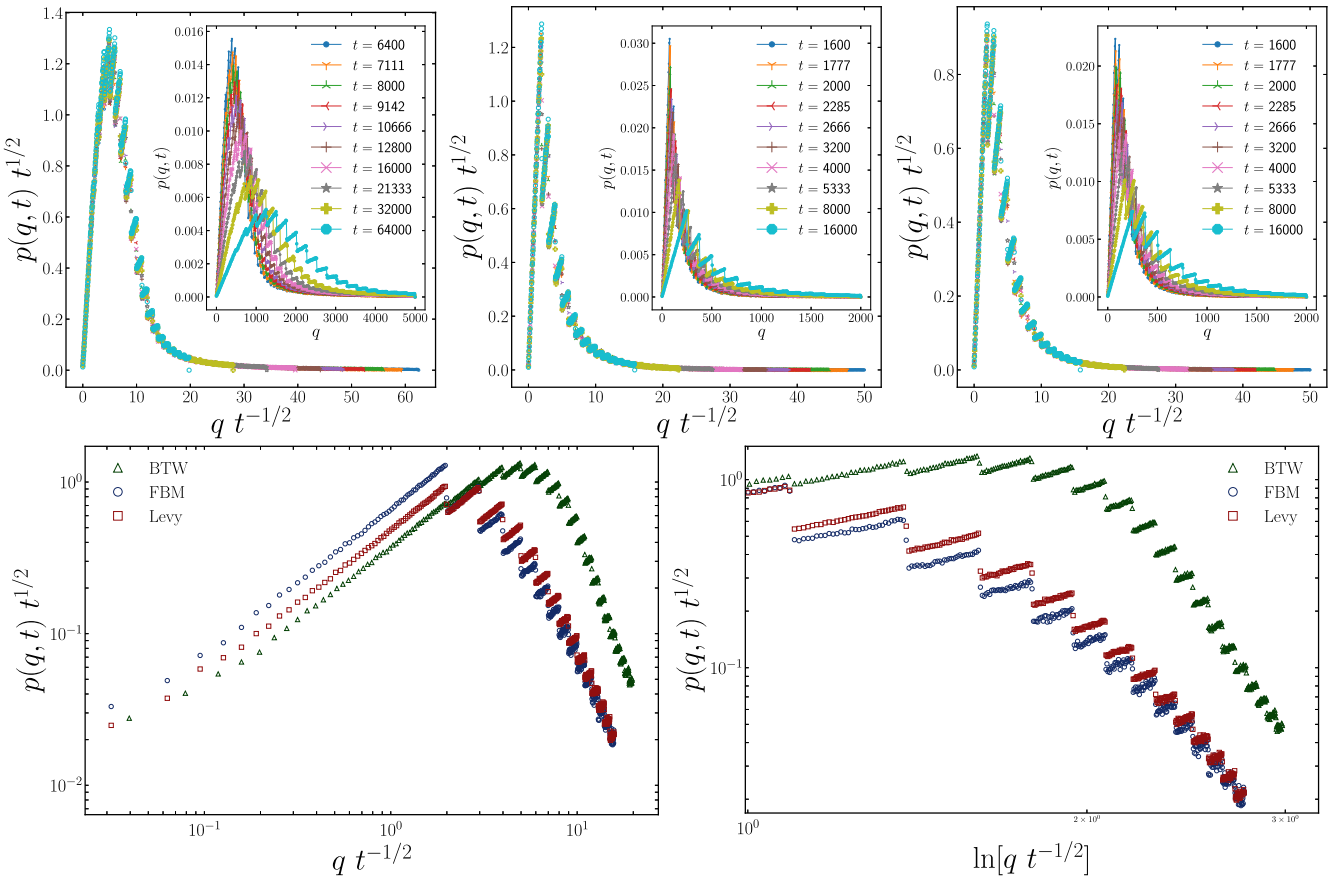

FIG. 3. (top row) Time-dependent probability distribution function of generalized degree for visibility graphs constructed from BTW model (left), FBM (middle), and Levy walks (right) time series. (bottom row) Changes on the behavior of generalized degree function $F(\xi)$ for various regimes (small ξ in left and large ξ in right) given by Eq. (21).

introducing a new exponent β. Our numerical estimation of these exponents are $\beta_{\rm BTW} = 0.50 \pm 0.03$, and $\beta_{\rm fBM}$ and $\beta_{\rm Levy}$ depend on H and α, respectively. Moreover, for the BTW model, $\lim_{L\to\infty} \eta_{\rm BTW} = 2.50 \pm 0.02$ for fixed maximum N, and $\lim_{N\to\infty} \eta_{\rm BTW} = 2.50 \pm 0.01$ for fixed maximum L. This serves as the first evidence of the failure of the Bathelemy's conjecture (C$\mathbb{I}$) [7], i.e., $\eta_{\rm BTW} > \eta_{\rm max}$. The clustering coefficient relation with the degree determines the hierarchical structure of a complex network. In addition to the Eq. (5), we have

$$c \propto k^{-\mu} \text{ and } b \propto c^{-\nu}, \tag{23}$$

resulting in

$$\eta = \mu\nu. \tag{24}$$

For the details of the associated fittings, see Fig. 4 for BTW (left), fBM (middle), and Levy (right). We observed that $\mu_{\rm BTW} = 0.956 \pm 0.002$ and $\nu_{\rm BTW} = 2.77 \pm 0.01 \approx \frac{\eta_{\rm BTW}}{\mu_{\rm BTW}}$ for BTW, $\mu_{\rm FBM} = \mu_{\rm FBM}(H)$, $\nu_{\rm FBM} = \nu_{\rm FBM}(H)$ for FBM and $\mu_{\rm Levy} = \mu_{\rm Levy}(\alpha)$, $\nu_{\rm Levy} = \nu_{\rm Levy}(\alpha)$, see Fig. 6 for details.

We also analyzed the probability distribution function (PDF) of k and b. The results are shown in the Fig. 5, the top row of which shows the PDF of degree for BTW (left), FBM (middle), and Levy walks (right) time series. We observed that the relation Eq. (4) indicating SF property is valid for all the models, with the exponent $\gamma_{\rm BTW} = 2.60 \pm 0.01$, $\gamma_{\rm FBM} = \gamma_{\rm FBM}(H)$ (decreasing function of H) and $\gamma_{\rm Levy} = \gamma_{\rm Levy}(\alpha)$ (increasing function of α). In the bottom row, the betweenness distribution functions is plotted for these models (with the same arrangement as the top row), revealing $\delta_{\rm BTW} = 1.71 \pm 0.02$, $\delta_{\rm FBM} = \delta_{\rm FBM}(H)$ and $\delta_{\rm Levy} = \delta_{\rm Levy}(\alpha)$ (increasing functions of H and α), see Fig. 6 for γ and δ in terms of α and H.

Figure 6 summarizes the numerical estimations of the critical exponents, calculated in the thermodynamics limit $N, L \to \infty$. The exponents run with H and α, in such a way that γ is a decreasing (an increasing) function of H (α) for fBM (Levy process) VGs. Our analysis shows that the best fitting to the numerical data in the limit $N \to \infty$ is $\gamma_{\rm FBM}(H) = (3.17 \pm 0.03) - (2.42 \pm 0.06)H$ for the fBM, which is in agreement with the previously observed relations [25,34]. The linear fitting of γ in terms of α reveals also that $\gamma_{\rm Levy}(\alpha) = (1.69 \pm 0.04) + (0.55 \pm 0.05)\,\alpha$ for the Levy process ($0.9 \leqslant \alpha \leqslant 1.6$), which is something new. The monotonic increase of γ in terms of α is understood given the fact that α controls the rare events in the Levy process, and rare events influence the visibility pattern of the nodes in VG. More precisely, α diminishes the abundance of rare events, which itself enhances the visibility conditions of the nodes, so that the degree of nodes with small k values increase, while it decreases for the nodes with large degrees (hubs), giving rise to an increase in γ, which is shown to be linear. Generally, one

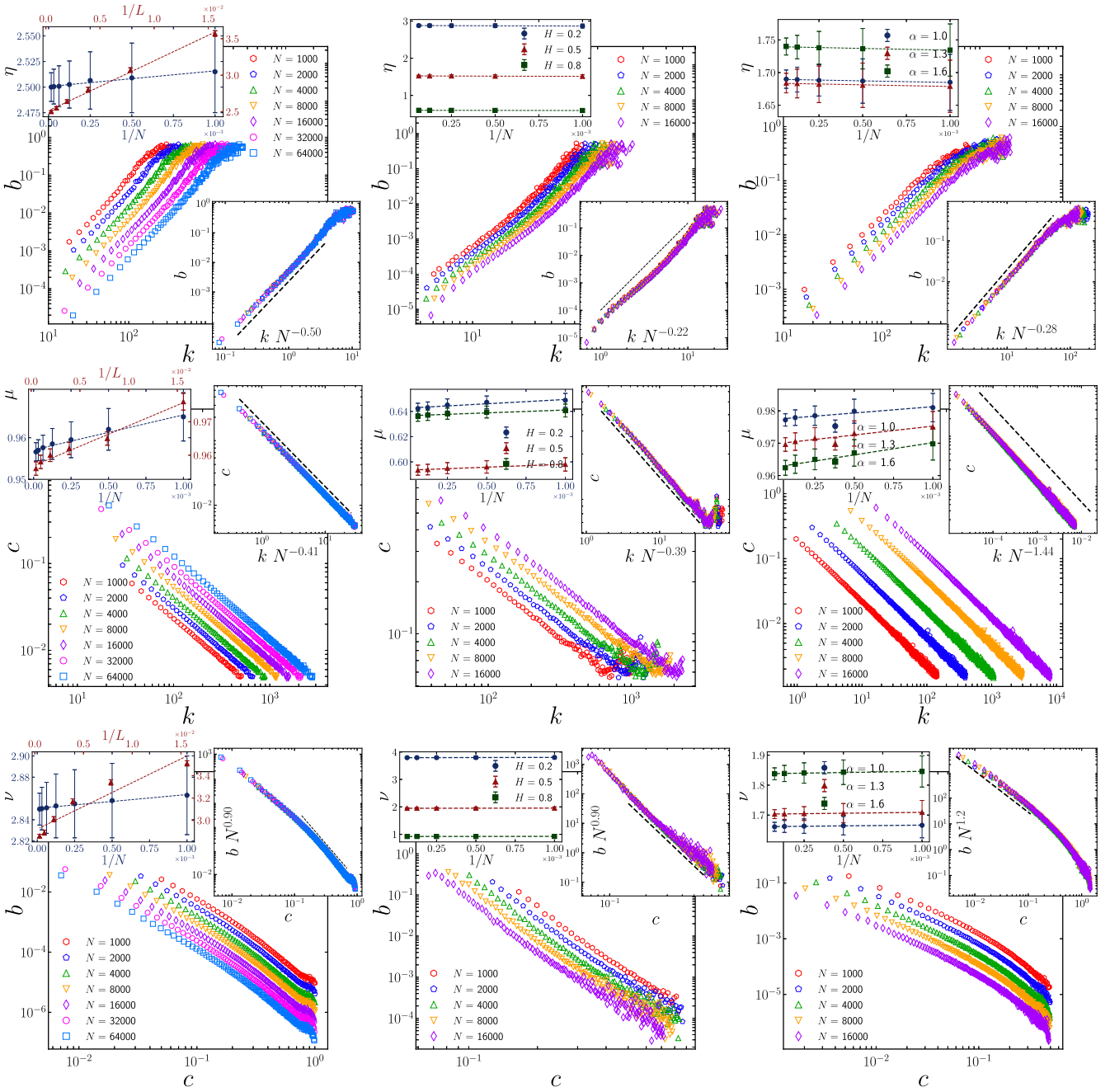

FIG. 4. (top row) Ensemble-averaged betweenness centrality versus the degree in log-log scale for VGs constructed from BTW model (left), FBM (middle), and Levy walks (right) time series. The top insets indicate size dependency of the exponent η (network size N and lattice size L for BTW model and N for the FBM series and Levy walk), while the bottom insets are showing the data collapse of the main plots. Correlation analysis of clustering coefficient versus degree (middle row) and betweenness centrality versus clustering coefficient (bottom row) of VG constructed from time series of BTW sandpile model (left column), FBM series (middle column), and Levy walk (right column) for different system size in log-log scale. The inset plots illustrate size dependency of the scaling exponent (left insets) and data collapse analysis (right insets).

expects that the betweenness increases by decreasing H since for small H values the VGs are more sparse. The exponent δ decreases with decreasing H, showing that this increase is smaller for the nodes with smaller betweenness than that for the nodes with larger betweenness. The same argument holds for α. In Fig. 6(c) the horizontal dashed-line shows the limit given by the Ref. [7], i.e., $\eta_{\max} = 2$ for SFTs. From this figure, we see that for fBM in the anticorrelated regime $0 < H \lesssim 0.5$, the conjecture of Eq. (7) (C$\mathbb{I}$) is violated, i.e., $\eta > \eta_{\max}$ just like the BTW model, while for the Levy process, η is always smaller than 2 for all α values in [0.9,1.6] in agreement with the conjecture.

We assert that the reason behind this considerable deviation from the Barthelemy's conjecture is the existence of large fluctuations in the scaling $b - k$ relation as first observed and pointed out in Refs. [9–11]. This phenomena leads to

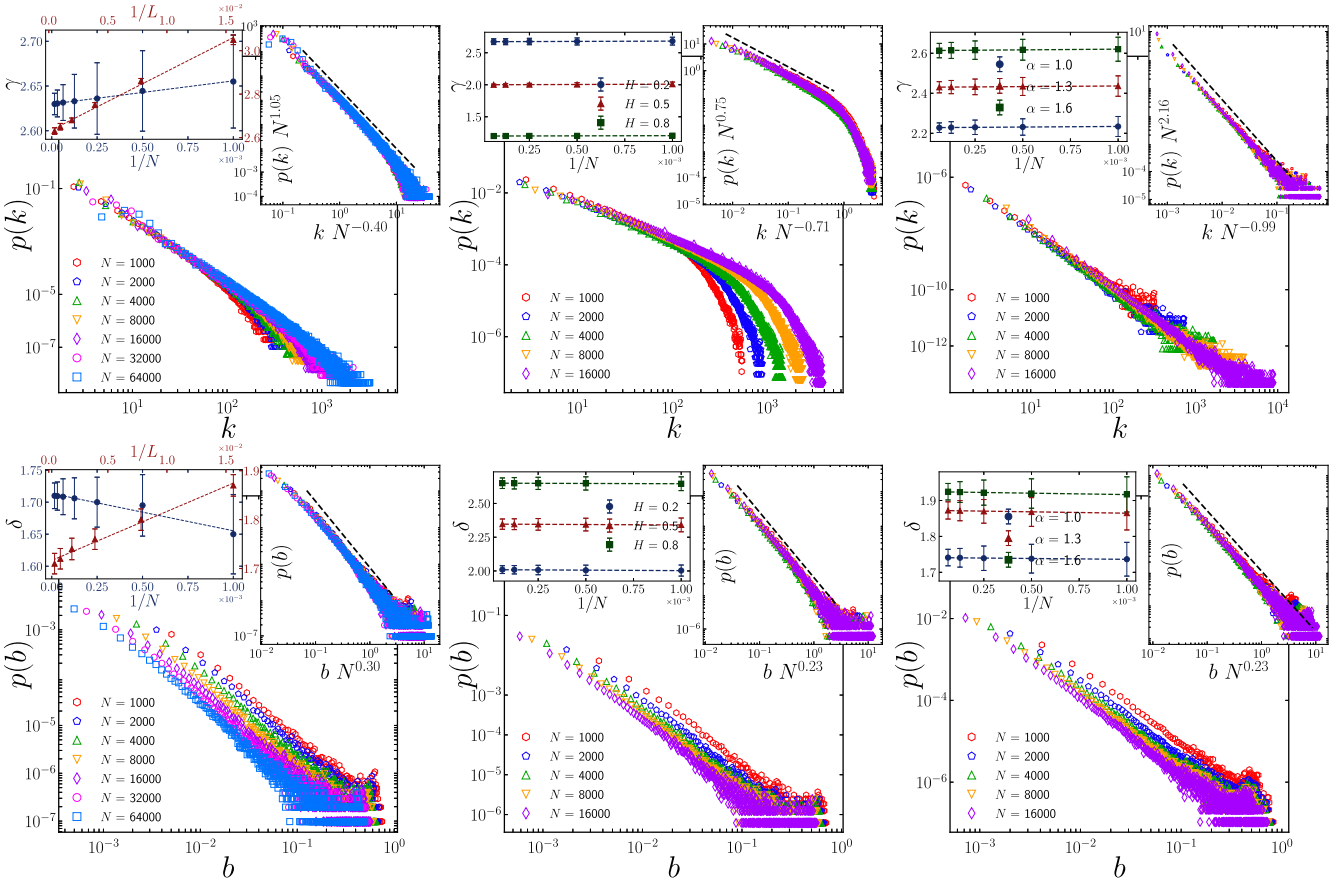

FIG. 5. Probability distribution function of degree (top row) and betweenness centrality (bottom row) of VG constructed from time series of various models studied in the work, BTW sandpile model (left column), FBM series (middle column), and Levy walk (right column) for different system size. The scaling behavior of these quantities reveals that the VGs are SF. The inset plots show size dependency of the scaling exponent (left insets) and data collapse analysis (right insets).

some peculiar consequences, like the violation of the hyperscaling relation Eq. (6), and also the fact that the highest degrees are typically not the most central ones in the sense of betweenness [9]. It is also responsible for the fractality observed in the synthetic and real-world SF networks [11]. For nonfractal networks, the degree and the betweenness centralities are strongly correlated, while in the fractal SF networks the betweenness centrality of low degree nodes in has the chance to be comparable to that of the hubs [11]. Such a large fluctuation is reflected in the conditional probability $p(b|k)$. Figure 7 shows $p(b|k = 10)$ in terms of b for the three cases. Interestingly, we see that this function decays in a power-law (heavy-tail) form for two cases BTW and fBM, while for the Levy process the situation is completely different: it decays exponentially with a finite width avoiding large fluctuations. The exponents for both power-law and exponential decays depend on the correlation parameter (H for fBM and α for Levy). Therefore, one concludes that the width of $p(b|k)$ is finite for the Levy process, the characteristic of the nonfractal SF network, while for the BTW and fBM it is diverging, leading to large fluctuations (a characteristic of fractal SF networks). The violation of the hyperscaling relation Eq. (6) for the BTW model and fBM (all H values) is shown in the upper graph in the Fig. 8, while the hyperscaling relation remains almost valid for the Levy process for all α values. For fBM, while the hyperscaling relation is violated for all H values, the Barthemly's conjecture [(C$\mathbb{I}$), see Fig. 8] fails only for $0 < H \lesssim 0.5$. Although Fig. 7 shows the fluctuations for the smaller values of H is higher (which favors the anomalous behavior), this issue needs more analysis which is beyond the scope of the present paper.

Before closing this section, it is worth adding notes on clustering coefficient, being a decreasing function of k in the real-world networks [38,39]. This decrease is a power law for nontree SF networks like the deactivation model ($\mu = 1$ [40]) and other generalized phenomenological models [41–43], while for the SF networks generated by preferentially attachments c and k are uncorrelated. For the Internet network, the exponents were found to be $\gamma = 2.2 \pm 0.1$ and $\delta = 2.1 \pm 0.2$, and also $\eta \approx 1$ and $\mu \approx 0.75 \pm 0.03$ [8], while for the actor network, language network, and WWW μ varies with γ. The Molloy and Reed (MR) algorithm and generalized BA (GBA) predicted that $\eta \approx 1$ and c does not depend on k [44,45], while for the fitness model $\eta \approx 1.4$ and c and b decay with k [46]. In Fig. 6(d) we show μ in terms of α and H for Levy and FBM processes respectively. For the former it is a decreasing function of α, while for the latter it is not monotonic, i.e., the clustering coefficient for hubs decreases leading to larger values for μ, which has not been observed previously. For low H values, the obtained μ is

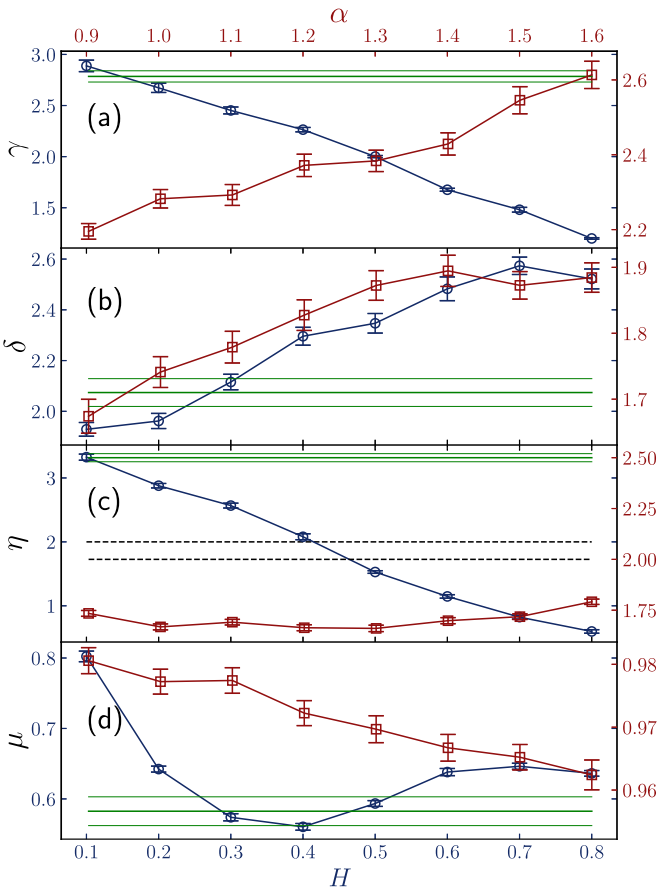

FIG. 6. The exponents (a) γ, (b) δ, (c) η, and (d) μ for the SF networks corresponding to three processes: the (green) lines show the BTW model and the error bars, the (blue) circles are for FBM, and the (red) square symbols show the Levy results. The left vertical axis shows the values for the FBM series, while the right-hand side vertical axis stands for the BTW model and the Levy walk. In the upper (lower) panel the horizontal axis α (H) is shown for the Levy walk (FBM series).

compatible with the values observed for the Internet network [8].

V. BETWEENNESS-DEGREE FLUCTUATIONS FOR THE GENERALIZED BARABASI-ALBERT MODELS

To be self-contained, it is worth inspecting the behavior of the fluctuations, and the validity of the Barthelemy's conjecture in other SF networks, although the main concentration of the paper is upon the VGs. The conditional distribution function $p(b|k)$ as a good measure for these fluctuations is considered here for the m-Barabasi-Albert (m-BA) model as a most popular SF network model with power-law scaling behavior. This model is recognized as a prototypical example of preferential attachment networks, which shares a plenty of behavior in common with natural networks, like the lack of an internal scale (as a necessary condition for SF networks) [47], with ($m > 1$) or without ($m = 1$) loops. The definition of the model is as follows: the nodes are added to the network one by one, starting from a single node at $t = 0$. Once a new node is added to the network, m new links are created to the

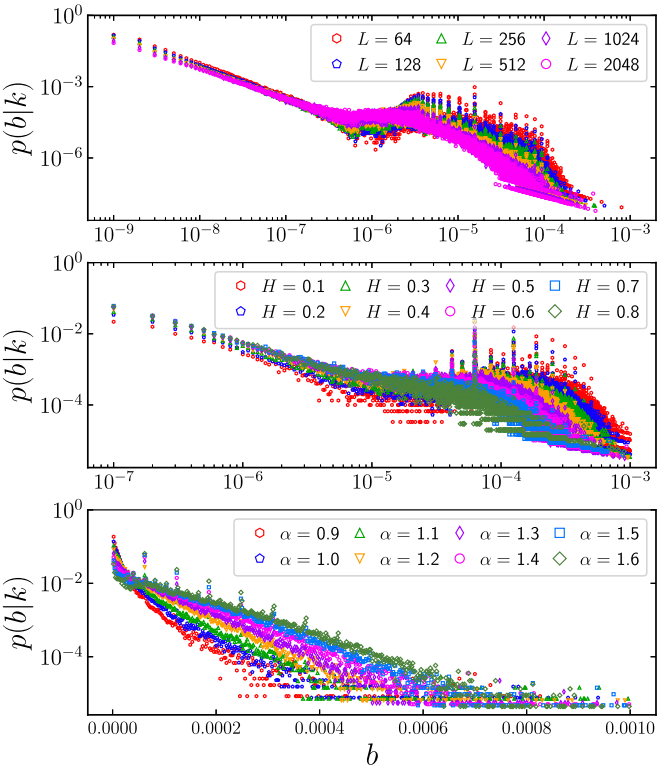

FIG. 7. The conditional probability distribution function $p(b|k)$ for various processes: BTW model (top panel), FBM series [$0.1 \leqslant H \leqslant 0.8$] (middle panel), and Levy walk [$0.9 \leqslant \alpha \leqslant 1.6$] (lower panel).

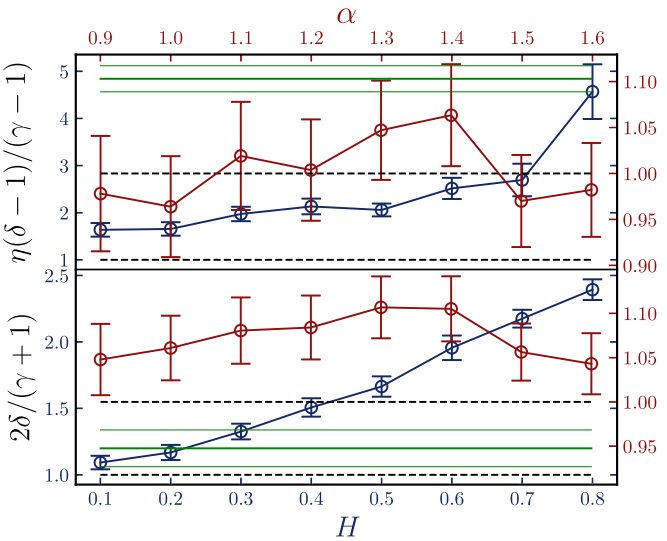

FIG. 8. (top panel) Hyperscaling relation analysis [Eq. (6)] for the BTW, the FBM and the Levy walk time series. The first two cases (the latter case) do not (do) satisfy Eq. (6). (lower panel) the inequality $\delta \geqslant \frac{\gamma+1}{2}$ is valid for Levy VG and FBM VG in the interval $H > 0.5$, while it is invalid for the BTW VG and FBM in the interval $H \lesssim 0.5$. The (green) lines show the BTW model and the error bars, the (blue) circles are for FBM, and the (red) square symbols show the Levy results. The left vertical axis is devoted for FBM and the right one is for both BTW and Levy.

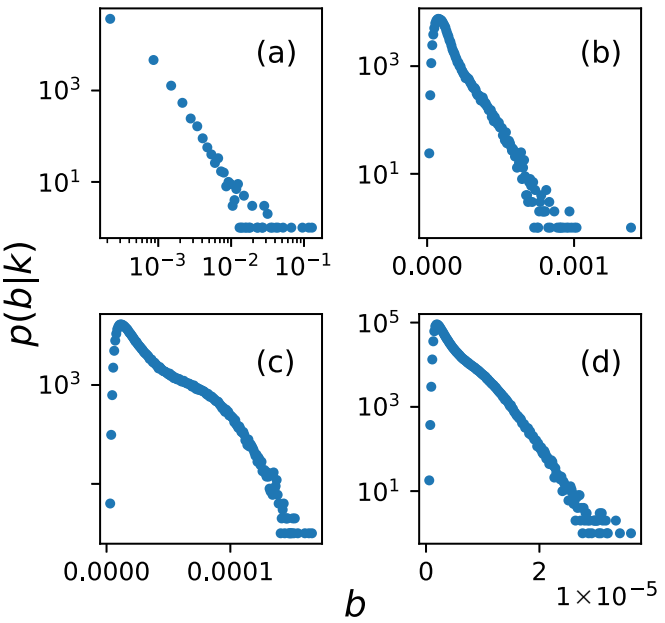

FIG. 9. $p(b|k)$ in terms of b for fixed $k = 8$ for m-BA model with (a) $m = 1$, (b) $m = 2$, (c) $m = 4$, and (d) $m = 8$. The scale of the vertical axis is logarithmic for all figures, but the scale is logarithmic for the horizontal axis for panel (a) and normal for the rest.

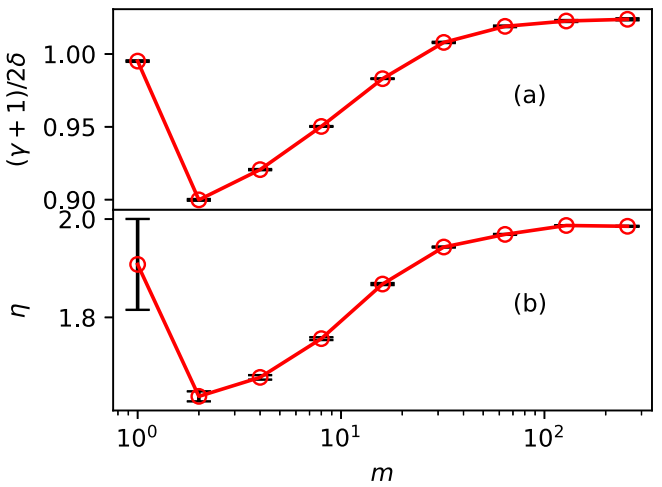

FIG. 10. (a) The validity of Eq. (7), for various amounts of m. We see that for $m = 1$, the equality part of the Eq. (7) is held ($\frac{\gamma+1}{2\delta} = 1$) up to some error bar. For other m values we have $\frac{\gamma+1}{2\delta} < 1$. (b) The same behavior for η is seen, and $\eta \leqslant 2$ as predicted by Barthelemy's conjecture.

newly generated node. The links are added probabilistically to the nodes with highest degrees. More precisely, the probability that a link is added to a node is proportional to its degree. In this network, the size of the network is the total time during which the network has formed. Many statistical properties of m-BA model has already been investigated in the literature, like the *clustering coefficient* defined as loops of order three ($m > 1$) [48,49], node degree correlations [50,51], and the absence of a *community structure* [52] and a hierarchical architecture [39]. To inspect the fluctuation statistics of m-BA model, we calculated and plotted $p(b|k)$ in terms of b (for fixed $k = 8$) in Fig. 9. We see that $p(b|k)$ decays exponentially with b for $m > 1$, while it is power law for $m = 1$ for almost two decades. The latter shows that the BA tree has large, fat tail $b - k$ fluctuations, satisfying *marginally* the Barthelemy's predictions [Eq. (7)]. With "marginally," we mean that the equalities hold for BA trees, which is realized from the exact values for the exponents $\gamma = 3$, $\delta = 2$, and $\eta = 2$, so that $\frac{\gamma+1}{2\delta} = 1$, and $\eta = 2$ (for $m = 1$ and $m > 1$ see Refs. [3,7,15,47,53,54]). Figure 10 shows $\frac{\gamma+1}{2\delta}$, and η in terms of m, which are compatible with the previous results (Table I and the references therein). The abrupt change of the conditional distribution function from power law ($m = 1$) to exponential decay ($m > 1$) leads directly to an abrupt change of exponents in this point. This is seen in the Fig. 10, where $\frac{\gamma+1}{2\delta}$, and η abruptly fall from their maximum values (1 and 2, respectively) when we move from $m = 1$ to $m > 1$ values. The exponents then grow as m increases and asymptotically approach those for the tree BA ($m = 1$ case) for $m \to \infty$.

We also calculated $f(k, \eta, x_b)$ given in Eq. (9) in the Fig. 11. We see that Eq. (8) holds for *all* m values, which is consistent with the above results, and show that Eq. (7) hold for all m values.

VI. CONCLUDING REMARKS

We considered the Barthelemy's conjecture for the betweenness-degree ($b - k$) scaling exponent for scale-free (SF) networks, which claims that $\eta_{\max} = 2$, belonging to scale-free trees (SFTs), based on which it was further conjectured that $\delta \geqslant \frac{\gamma+1}{2}$. We analyzed the VGs for the time series of 2D BTW model, 1D fBM (controlled by the Hurst exponent H) and 1D Levy walks (controlled by the step index α). We numerically showed that the VGs for all of these models are SF, with well-defined scaling exponents. A superuniversal behavior is found for the distribution function for generalized degree function $p(q, t)$ identical to Barabasi-Albert network, see Eq. (19). We present evidence for violation of Barthelemy's conjecture. Specifically for the BTW model and FBM with $H \lesssim 0.5$, η is larger than 2, and also for the BTW

TABLE I. The exponents of m-BA model, adopted from Refs. [3,7,47]. The last row concerns that validity of Eq. (7).

	$m = 1$	$m = 2$	$m = 3$	$m = 4$	$m = 5$	Ref.
γ	3 (analytic)	3 (analytic)	3 (analytic)	3 (analytic)	2.9 ± 0.1 and analytically 3	[47]
δ	2 (analytic)	2.3 ± 0.1 ($N = 10^4$) ≈ 2.17	≈ 2.17			[3,15,53]
η	2 (analytic)	1.81 ± 0.02 ($N = 5 \times 10^4$)				[7,15,54]
$(\gamma + 1)/2\delta$	1	<1.0	<1.0			

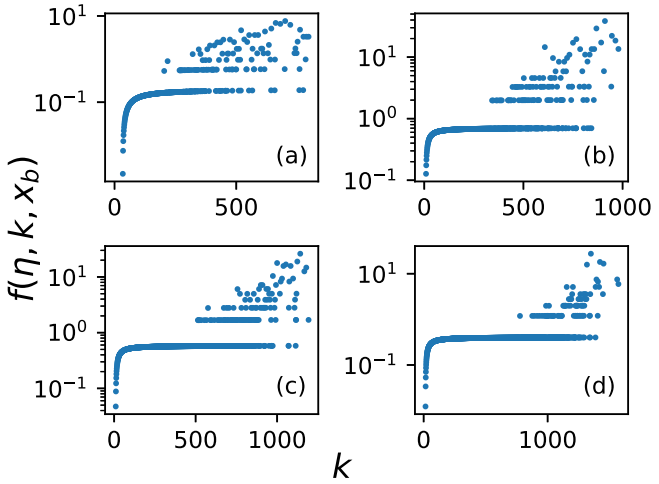

FIG. 11. $f(\eta, k, x_b)$ in terms of k for m-BA model for $N = 64000$ and for (a) $m = 1$, (b) $m = 2$, (c) $m = 4$, and (d) $m = 8$.

model $\delta < \frac{\gamma+1}{2}$, while the Barthelemy's conjecture remains valid for the Levy process for all α values. By analyzing the conditional probability $p(b|k)$ we argue that the failure of Barthelemy's conjecture is due to the large fluctuations (or uncertainty) in the $b-k$ scaling relation. This function decays in a power-law fashion for the BTW model as well as the FBM for all H values. This results further in a violation of hyperscaling relation $\eta = \frac{\gamma-1}{\delta-1}$ and as a result of some emergent anomalous behavior for the BTW model and FBM series.

In the last part of the paper we considered the m-BA model to test the formalism that we developed in the first part of the paper. We chose m-BA model because of its vast applications in SF networks. We calculated $p(b|k)$ as a function of b and k. For $m = 1$ this function is a power law, while for $m > 1$ it decays exponentially, making BA tree very especial. Then we calculated $\frac{\gamma+1}{2\delta}$ and η in terms of m (Fig. 10), showing that the Barthelemy's conjecture works for all m values. An abrupt change of exponents takes place when one moves from $m = 1$ to $m > 1$ in accordance with the change of behavior for $p(b|k)$. Equation (8) for $f(\eta, k, x_b)$ was tested for various m values, confirming that this equation (and also Barthelemy's conjecture) is valid for m-BA model.

APPENDIX: BARTHELEMY'S IDENTITIES

Barthelemy's equation imply an additional strong restriction to k, b, and $p(b)$ for large enough k and b values. To see this, we expand the Eq. (4) to the first order of $1/k$ and $1/b$, so that

$$\gamma = k(1 - x_k), \quad \delta\eta = k(1 - x_b), \tag{A1}$$

where $x_k \equiv \frac{p(k+1)}{p(k)}$, $x_b \equiv \frac{p(b')}{p(b)}$, and $b' = b_{k+1}$. Then (CIII) in the Eq. (7) gives

$$2k(1 - x_b) \geqslant \eta[k(1 - x_k) + 1]. \tag{A2}$$

On the other hand, by expanding the following equation up to the first order of $1/k$ and $1/b$

$$p(k) = p(b)\frac{db}{dk} = \eta\frac{b}{k}p(b), \tag{A3}$$

and also

$$p(k+1) = p(b')\eta\frac{b'}{k+1} \approx p(b')\eta\frac{b}{k}\left[1 + \frac{\eta-1}{k}\right], \tag{A4}$$

so that

$$x_k = \frac{p(k+1)}{p(k)} = x_b\left[1 + \frac{\eta-1}{k}\right]. \tag{A5}$$

Inserting this into Eq. (A2) one finds

$$f(\eta, k, x_b) \geqslant 0, \tag{A6}$$

where

$$f(\eta, k, x_b) \equiv x_b\eta^2 - [k + 1 - (k-1)x_b]\eta + 2k(1 - x_b). \tag{A7}$$

This function has been shown in Fig. 1 for two different k values. To find the analytical form of solution, we find the roots of $f(\eta, k, x_b)$, which are

$$\eta_*^{\pm} = (2x_b)^{-1}[B \pm \sqrt{B^2 + 8kx_b(1 - x_b)}],$$
$$B = k + 1 - (k-1)x_b. \tag{A8}$$

Then the possible solutions are

$$\begin{cases} \eta > \eta_*^{(+)} \\ \eta < \eta_*^{(-)}, \end{cases} \text{combined with } \eta \leqslant 2. \tag{A9}$$

The upper branch ($\eta_*^{(+)}$) grows linearly with k for large enough k values, while the lower branch saturates to $\eta_*^{(-)} \to 2$. Therefore, for $k \to \infty$, the solution $\eta < 2$ is the exact solution as expected. To see this more directly, notice that

$$f(\eta, k, x_b)|_{k\to\infty} \to k(1 - x_b)(2 - \eta), \tag{A10}$$

so that $f(\eta, k, x_b) \geqslant 0$ (noting that $0 < x_b < 1$) gives $\eta \leqslant 2$. As another example, consider the case η is about 2, i.e., $\eta = 2^-$, where Eq. (A6) for finite and large k values imply that [to $O(k^{-2})$]

$$\frac{1}{x_b} \leqslant \eta - 1 < 1. \tag{A11}$$

Therefore, the prediction of the Barthelemy's conjecture in this case (η close to two) is

$$x_b \geqslant \frac{1}{\eta - 1}. \tag{A12}$$

[1] L. d. F. Costa, F. A. Rodrigues, G. Travieso, and P. R. Villas Boas, Adv. Phys. **56**, 167 (2007).

[2] K.-I. Goh, B. Kahng, and D. Kim, Phys. Rev. Lett. **87**, 278701 (2001).

[3] K.-I. Goh, E. Oh, H. Jeong, B. Kahng, and D. Kim, Proc. Natl. Acad. Sci. USA **99**, 12583 (2002).
[4] G. Yan, T. Zhou, B. Hu, Z.-Q. Fu, and B.-H. Wang, Phys. Rev. E **73**, 046108 (2006).
[5] G. Szabó, M. Alava, and J. Kertész, Phys. Rev. E **66**, 026101 (2002).
[6] H. Wang, J. M. Hernandez, and P. V. Mieghem, Phys. Rev. E **77**, 046105 (2008).
[7] M. Barthelemy, Eur. Phys. J. B **38**, 163 (2004).
[8] A. Vázquez, R. Pastor-Satorras, and A. Vespignani, Phys. Rev. E **65**, 066130 (2002).
[9] R. Guimera and L. A. N. Amaral, Eur. Phys. J. B **38**, 381 (2004).
[10] A. Barrat, M. Barthélemy, and A. Vespignani, J. Stat. Mech. (2005) P05003.
[11] M. Kitsak, S. Havlin, G. Paul, M. Riccaboni, F. Pammolli, and H. E. Stanley, Phys. Rev. E **75**, 056115 (2007).
[12] J. Sienkiewicz and J. A. Hołyst, Phys. Rev. E **72**, 046127 (2005).
[13] M. Barthélemy, Phys. Rep. **499**, 1 (2011).
[14] K.-I. Goh, C.-M. Ghim, B. Kahng, and D. Kim, Phys. Rev. Lett. **91**, 189804 (2003).
[15] M. Barthélemy, Phys. Rev. Lett. **91**, 189803 (2003).
[16] B. Aguilar-San Juan and L. Guzman-Vargas, Eur. Phys. J. B **86**, 454 (2013).
[17] H. Masoomy, B. Askari, M. N. Najafi, and S. M. S. Movahed, Phys. Rev. E **104**, 034116 (2021).
[18] W.-J. Xie and W.-X. Zhou, Phys. A: Stat. Mech. Appl. **390**, 3592 (2011).
[19] L. Lacasa, B. Luque, F. Ballesteros, J. Luque, and J. C. Nuno, Proc. Natl. Acad. Sci. USA **105**, 4972 (2008).
[20] L. Rong and P. Shang, Nonlinear Dyn. **92**, 41 (2018).
[21] A. Braga, L. Alves, L. Costa, A. Ribeiro, M. De Jesus, A. Tateishi, and H. Ribeiro, Phys. A (Amsterdam, Neth.) **444**, 1003 (2016).
[22] J. Wang, C. Yang, R. Wang, H. Yu, Y. Cao, and J. Liu, Phys. A: Stat. Mech. Appl. **460**, 174 (2016).
[23] G. Zhu, Y. Li, P. P. Wen, and S. Wang, Brain Inf. **1**, 19 (2014).
[24] M. Zheng, S. Domanskyi, C. Piermarocchi, and G. I. Mias, Sci. Rep. **11**, 5623 (2021)
[25] L. Lacasa, B. Luque, J. Luque, and J. C. Nuno, Europhys. Lett. **86**, 30001 (2009).
[26] R. Dickman, M. Alava, M. A. Muñoz, J. Peltola, A. Vespignani, and S. Zapperi, Phys. Rev. E **64**, 056104 (2001).
[27] P. Bak and C. Tang, J. Geophys. Res. **94**, 15635 (1989).
[28] P. Charbonneau, S. W. McIntosh, H.-L. Liu, and T. J. Bogdan, Sol. Phys. **203**, 321 (2001).
[29] D. L. Turcotte and B. D. Malamud, Phys. A: Stat. Mech. Appl. **340**, 580 (2004).
[30] M. N. Najafi, J. Cheraghalizadeh, and H. J. Herrmann, Phys. Rev. E **103**, 052106 (2021).
[31] M. N. Najafi, J. Cheraghalizadeh, M. Luković, and H. J. Herrmann, Phys. Rev. E **101**, 032116 (2020).
[32] M. Najafi, S. Tizdast, and J. Cheraghalizadeh, Phys. Scr. **96**, 112001 (2021).
[33] I. Nourdin and R. Zintout, arXiv:1311.2895.
[34] X.-H. Ni, Z.-Q. Jiang, and W.-X. Zhou, Phys. Lett. A **373**, 3822 (2009).
[35] D. Applebaum, *Lévy Processes and Stochastic Calculus* (Cambridge University Press, Cambridge, UK, 2009).
[36] K. Arias-Calluari, F. Alonso-Marroquin, and M. S. Harré, Phys. Rev. E **98**, 012103 (2018).
[37] M. K. Hassan, M. Z. Hassan, and N. I. Pavel, J. Phys. A: Math. Theor. **44**, 175101 (2011).
[38] A. Vázquez, M. Boguná, Y. Moreno, R. Pastor-Satorras, and A. Vespignani, Phys. Rev. E **67**, 046111 (2003).
[39] E. Ravasz and A.-L. Barabási, Phys. Rev. E **67**, 026112 (2003).
[40] K. Klemm and V. M. Eguiluz, Phys. Rev. E **65**, 036123 (2002).
[41] A.-L. Barabási, E. Ravasz, and T. Vicsek, Phys. A: Stat. Mech. Appl. **299**, 559 (2001).
[42] S. N. Dorogovtsev, A. V. Goltsev, and J. F. F. Mendes, Phys. Rev. E **65**, 066122 (2002).
[43] S. Jung, S. Kim, and B. Kahng, Phys. Rev. E **65**, 056101 (2002).
[44] M. Newman, A.-L. Barabási, and D. J. Watts, in *The Structure and Dynamics of Networks* (Princeton University Press, 2006).
[45] R. Albert and A.-L. Barabási, Phys. Rev. Lett. **85**, 5234 (2000).
[46] G. Bianconi and A. L. Barabási, EPL **54**, 436 (2001).
[47] A.-L. Barabási and R. Albert, Science **286**, 509 (1999).
[48] M. E. Newman, SIAM Rev. **45**, 167 (2003).
[49] M. E. J. Newman, Phys. Rev. E **64**, 016131 (2001).
[50] P. L. Krapivsky and S. Redner, Phys. Rev. E **63**, 066123 (2001).
[51] M. Boguná and R. Pastor-Satorras, Phys. Rev. E **66**, 047104 (2002).
[52] S. Fortunato, Phys. Rep. **486**, 75 (2010).
[53] J. Lee, Y. Lee, S. M. Oh, and B. Kahng, Chaos **31**, 061108 (2021).
[54] O. Narayan and I. Saniee, Phys. Rev. E **82**, 036102 (2010).